View metadata, citation and similar papers at core.ac.uk

brought to you by CORE

provided by Infoscience - École polytechnique fédérale de Lausanne

Elsevier Editorial System(tm) for Applied Thermal Engineering
Manuscript Draft

Manuscript Number:

Title: Numerical simulations of a prechamber autoignition cogeneration engine operating on natural gas

Article Type: Research Paper

Section/Category:

Keywords: autoignition; prechamber; cogeneration; computational fluid dynamics

Corresponding Author: Mr Stefan Heyne, MSc

Corresponding Author's Institution: Energy and Environment

First Author: Stefan Heyne, MSc

Order of Authors: Stefan Heyne, MSc; Grégory Millot; Daniel Favrat, Professor

Manuscript Region of Origin:

Abstract: A numerical simulation of a prechamber autoignition gas engine has been performed based on an experimental test case. With a simplified finite-rate/eddy-dissipation model for the combustion of natural gas, it was possible to properly reproduce the experiment considering the combustion duration, ignition timing and overall energy balance. However the predefined empiric constant of the eddy-dissipation model had to be increased by a factor of 10. A modification of the original cylindrical-conical prechamber geometry to a simpler cylindrical one was tested with the simulation model. The influence of burnt gases inside the prechamber was assessed simulating the mixture formation inside the prechamber. The simulations showed little effect of taking into account the non-homogeneities in the gas phase on the combustion duration. The simulation showed that the new and cylindrical geometry envisaged did not show any improvement in the combustion homogeneity inside the prechamber and its volume (limited by the real engine geometry) is in fact not sufficient to properly ignite the main chamber. The model can be used to further guide design modifications of the prechamber engine to improve performance.

Manuscript

# Numerical simulations of a prechamber autoignition cogeneration engine operating on natural gas

S. Heyne, G. Millot and D. Favrat *

[a] *Industrial Energy Systems Laboratory, Ecole Polytechnique Fédérale de Lausanne, 1015 Lausanne, Switzerland*

**Abstract**

A numerical simulation of a prechamber autoignition gas engine has been performed based on an experimental test case. With a simplified finite-rate/eddy-dissipation model for the combustion of natural gas, it was possible to properly reproduce the experiment considering the combustion duration, ignition timing and overall energy balance. However the predefined empiric constant of the eddy-dissipation model had to be increased by a factor of 10. A modification of the original cylindrical-conical prechamber geometry to a simpler cylindrical one was tested with the simulation model. The influence of burnt gases inside the prechamber was assessed simulating the mixture formation inside the prechamber. The simulations showed little effect of taking into account the non-homogeneities in the gas phase on the combustion duration. The simulation showed that the new and cylindrical geometry envisaged did not show any improvement in the combustion homogeneity inside the prechamber and its volume (limited by the real engine geometry) is in fact not sufficient to properly ignite the main chamber. The model can be used to further guide design modifications of the prechamber engine to improve performance.

*Key words:* autoignition, prechamber, cogeneration, computational fluid dynamics
*PACS:* 07.20 Pe

## 1 Introduction

A prechamber autoignition concept for stationary cogeneration engines is currently being developed at the Industrial Energy Systems Laboratory (LENI). To better understand and guide the experimental work, a numerical simulation of the experimental set-up has been performed. Autoignition in an engine being strongly dependent on local conditions, direct coupling between computational fluid dynamics and chemistry was applied to have a high resolution of the computational domain. The engine concept under development is based on former work on unscavanged prechamber ignition with spark plugs where fluid dynamics simulations were successfully used to optimise the prechamber shape. The efficiency of the engine concept to reduce emissions below the Swiss emission limits for stationary for both natural gas and biogas was demonstrated [1–3]. The new engine concept is based on autoignition of the gas mixture inside a heated unscavanged prechamber. Through the temperature control of a limited volume (prechamber) the concept can be considered to be similar as, but easier to control than homogeneous charge compression ignition (HCCI), an engine concept with very low $NO_x$ emissions. The potential of this new prechamber autoignition concept has been demonstrated by experimental studies [4].

* Corresponding author.
*Email address:* daniel.favrat@epfl.ch (D. Favrat).

Numerical studies with varying levels of detail have been extensively used to study HCCI combustion. Aceves et al. [5] have validated a multi-zone model on an HCCI engine operating with propane. Heat release rate, HC and CO emissions as well as pressure traces were predicted with good agreement. Kong [6] studied natural gas/DME HCCI combustion using CFD with detailed chemistry. Combustion and operation limits of the engine as well as the influence of the fuel composition were well reproduced by the simulations. Zheng et al. [7] simulated a prechamber autoignition engine with direct injection of natural gas using the GRI3.0 reaction mechanism [8]. The engine concept studied in this paper is different from their concept in the fact that air and fuel are mixed prior to admission in the engine and no pilot injection into the prechamber is used. Ignition is triggered inside the prechamber by means of a resistive heating of the prechamber walls. As a numerical study using detailed chemistry proved difficulties in convergence and was very intensive in calculation time [9], a simplified combustion model implemented in the commercial code Fluent is used in this work. The mixture formation as well as changes in the prechamber geometry are investigated.

## 2 Simulation

To simplify simulations, the valves are not represented and a closed system is modelled. During the experiment, the inlet valve is closed at 130 °CA before top dead centre (BTDC) only, but in order to account for the gas motion due to the piston movement, simulations are started at bottom dead centre (BDC). The geometry is reduced to one quarter of the cylinder given the periodicity imposed by the four nozzle orifices of the prechamber. The mesh is made up

of hexahedral cells. The piston movement is controlled by a slider-crank shaft law and the mesh is updated using the Layering method, adding or deleting mesh layers from a surface of the dead volume. The mesh size decreases from 400 000 to 200 000 during compression and increases up to 480 000 during expansion as illustrated in Fig. 1. The simulations presented in this paper represent five different cases (1). Two different prechamber geometries were investigated: the original cylindrical-conical prechamber shape (geometry 1) used during the experiments and a simpler cylindrical one (geometry 2). The two shapes are illustrated in Fig. 2. There is no notable difference in the mesh for the two prechamber geometries simulated. In a previous study it has been shown that the temperature distribution in the original prechamber is too stratified to obtain a homogeneous ignition [9]. Therefore a new geometry, constrained by the real engine cylinder head geometry was tested. The volume of geometry 2 is 490 $mm^3$ compared to 1630$mm^3$ for geometry 1. The engine dimensions and simulated experimental conditions are given in Table 1. For further information the reader is referred to [4].

In order to investigate the mixture formation for both geometries, non-reactive simulations have been run, assuming burnt gases inside the prechamber and a mixture of fresh gases and burnt gases in the main chamber. Subsequent, reactive calculations for both geometries, assuming a homogeneous gas phase, have been run for both geometries, and one simulation taking into account combustion and mixture formation for the original prechamber geometry. In the following, the simulations will be referred to as indicated in Table 2.

The chemistry is represented by a global reaction model for natural gas represented by methane, ethane and propane. The composition of the gas is known from the experiments and higher hydrocarbons have been neglected. It has

been shown that a good representation of natural gas combustion is feasible with this simplification [10]. To model combustion chemistry, the Fluent model finite-rate/eddy-dissipation is used. The reaction rate is both calculated based on an finite-rate Arrhenius model (FR) and an eddy-dissipation model (ED) developed by Magnussen and Hjertager [11], the smaller of both values being kept. The reaction rate of the species $i$ is $R_i = \sum_r \min\left(R_{i,r}^{FR}, R_{i,r}^{ED}\right)$ where:

$$R_{i,r}^{FR} = M_i \left(\nu_{i,r}^{''} - \nu_{i,r}^{'}\right) \prod_j \left[C_{j,r}\right]^{\left(\eta_{j,r}^{'} + \eta_{j,r}^{''}\right)} A_r T^{\beta_r} e^{-\frac{E_{a,r}}{RT}} \tag{1}$$

$$R_{i,r}^{ED} = \nu_{i,r}^{'} M_i A \rho \frac{\epsilon}{k} \min\left(\min_R \left(\frac{Y_R}{\nu_{R,r}^{'} M_R}\right), B \frac{\sum_P Y_P}{\sum_j^N \nu_{j,r}^{''} M_j}\right) \tag{2}$$

with $M_i$ the molar mass of species $i$, $\nu_{i,r}^{'}$ and $\nu_{i,r}^{''}$ the stoichiometric coefficient for the reactant respectively product $i$ for reaction $r$, $C_j$ the molar concentration of species $j$ in reaction $r$, $\eta_{j,r}^{'}$ and $\eta_{j,r}^{''}$ the rate exponents for reaction respectively product species $j$ in reaction $r$, $A_r$ the pre-exponential factor for reaction $r$, $\beta$ the temperature exponent, $E_a$ the activation energy and $R$ the universal gas constant. For the eddy dissipation model, $A$ and $B$ denote empiric constants, $Y_P$ the mass fraction of any product species $P$, $Y_R$ that of a particular reactant $R$. $\epsilon$ represents the turbulent dissipation rate and $k$ the kinetic energy. Due to the relatively low temperature before ignition, it is the Arrhenius law that controls chemistry and determines autoignition whereas the EDC controls the flame speed during combustion. The empirical constant $A$ of the EDC is generally set to a numeric value of 4 ([11]). Based on the combustion duration of the experiment this value was adjusted and increased by a factor of 10. This adaption is consistent with other work where the value of both A and B have been increased by a factor of 8 for simulating turbulent premixed flames [11]. The $k\epsilon$-Realizable model and standard wall functions

are used to model turbulence. Thermal effects in the diffusion equation are neglected. The Fluent database values are used for parameters of Arrhenius laws and polynomial interpolations of heat capacities.

The boundary conditions to be specified are the wall temperature for both prechamber and main chamber. The prechamber temperature is measured by a thermocouple during the experiments. For the main chamber, based on a heat balance taking into account the cooling circuit, the mean temperature of the cylinder gases and the heat transfert coefficients and a mean wall temperature. The latter had been evaluated during a former work [9]. Initial conditions include mixture composition, pressure, temperature and level of turbulence. Two different cases simulated have to be considered here. Simulations with homogeneous composition all over the gas phase (simulations R1 and R3) simply use the mixture composition calculated based on the relative air-to-fuel ratio $\lambda = 1.31$ from the experiments and the burnt gases left in the dead volume. When taking into account the mixture formation inside the prechamber (simulations D1,D2 and R2), it is assumed that the gases inside the prechamber are initially composed of burnt gases only. For the main chamber the same mixing rule as for the homogeneous cases applies. The initial pressure for the simulations could not be based on the measured value as the signal is very noisy at BDC due to the valve motion and the induced pressure fluctuations. In addition, it has to be accounted for the fact, that during the experiment the valves are only closing at 130°CA BTDC. Therefore, this value is calculated for an adiabatic compression in order to obtain the experimental value of maximum pressure for a motored cycle without combustion, assuming that the pressure at BDC is not very dependant on the intake gas composition. Once composition, pressure and trapped mass are known, the temperature

is obtained by the ideal gas law. For simulations D1, D2 and R2, the temperature of the gases inside the prechamber is assumed to be equal to the experimentally measured exhaust gas temperature. The level of initial turbulence is based on literature and preliminary simulations. A summary of the boundary and initial conditions for the different simulations is given in Table 3.

## 3 Results

The investigation of mixture formation for the two geometries showed that the original prechamber shape results in a very homogeneous distribution considering the relative air-to-fuel ratio $\lambda$. Fig. 3 shows the range of $\lambda$ at 27°CA BTDC in a cut plane of the prechamber and illustrates well that the maximal value of $\lambda$ for geometry 1 is about 1.6 in the top centre region of the prechamber. For geometry 2 little mixing of the burnt gases and the fresh gases occurs and the burnt gases are actually only compressed at the top of the prechamber. The $\lambda$ value exceeds 2 in the top of the prechamber. The relative air-to-fuel ratio being an important parameter for ignition timing, the original geometry seems more favourable for homogeneous ignition. The main reason for the bad mixing for geometry 2 is the fact that the swirl motion - induced by the holes connecting prechamber and main chamber which are inclined by 10° in the radial direction - dies out due to the constant small prechamber diameter. For the original prechamber shape it is mainly this swirl that renders the mixture more homogeneous. In addition, a stronger effect of recirculation for geometry 1 enhances the mixing.

The reactive calculations all showed good agreement with the experimental

ignition timing and combustion duration. Table 4 illustrates that the moment of 5% heat release $\theta_{5\%}$ coincides acceptably well with the experimental data for the two simulations R1 and R2. Simulation R2, taking into account the mixture formation in the prechamber shows a particularly good agreement. The same applies for the combustion duration. Simulation R3 results in an earlier ignition and a longer combustion duration. The parameter $\Delta_{ignition}$ in Table 4 represents the delay between the complete ignition of the prechamber, indicated by a small pressure peak, and the moment of 5% heat release in the main chamber. It can be interpreted as a measure of the capability of the prechamber to ignite the main chamber. It can be seen that for geometry 2, the value is more than 3 times higher compared to geometry 1. This indicates that the volume of geometry 2 is not sufficient to rapidly ignite the main chamber.

The fact that the volume of the new prechamber geometry is not sufficient to properly ignite the main chamber can also be observed in Fig. 4, illustrating the flame front at 5% heat release for each simulation. For simulation R3 it shows that the jets issuing from the prechamber are not penetrating deep enough into the main chamber to properly ignite the mixture. The combustion in the main chamber in consequence is rather controlled by the heating due to compression than by the prechamber jets. Comparing simulations R1 and R2 it can be observed that for the homogenous gas phase simulation R1, the jets are penetrating deeper into the main chamber. This results in consequence in a slightly shorter combustion duration. Due to the higher fuel concentration inside the prechamber, the energy release is higher and the velocity of the gases leaving the prechamber is more elevated compared to simulation R2. The differences in the overall combustion duration $\Delta_{combustion}$ are negligible

between the two simulations. It has to be mentioned that for all simulations - as for the experiment - the ignition timing is very early. This could be influenced by reducing the prechamber wall temperature in order to shift ignition closer to TDC.

A comparison of the pressure traces for simulations R1 and R2 with the measured pressure trace illustrated in Fig. 5 shows that the peak pressure is over predicted by both simulations. Simulation R2 results in a lower peak pressure indicating the necessity of taking into account the mixture inhomogeneities for the simulations. The over prediction of the pressure in the simulations resides in the fact that pressure losses due to crevice flow are not modelled. In addition the combustion is complete for both simulations whereas during the experiment a non-negligible amount of unburned hydrocarbons is measured. A comparison of the experimental case and simulation R2 considering the energy balance is illustrated in Table 5. As only the compression and combustion phase are modelled, it is not possible to detail the heat flux $\dot{Q}_{total}$ and the energy flux leaving with the exhaust gases $\dot{E}_{exhaust}$ for the simulation. The sum of both results from the calculation of the overall energy balance. It can be seen that for both the experiment and simulation, the order of magnitude given in literature [12] are attained. This holds except for the high value of unburned hydrocarbons measured in the experiments. An engine geometry specifically designed for the prechamber concept would be necessary to reduce this value. Based on the simulations, an instantaneous energy balance was established as shown in Fig. 6. The very low imbalance in the overall energy balance shows that the simulation is well in accordance with the real case. Small deviations are noted during the combustion process that can be attributed to numerical instabilities. Both the overall and instantaneous energy balance can be used

to further validate the model based on experimental measurements.

## 4 Conclusions

A numerical model for the simulation of a compression and combustion cycle for a prechamber autoignition has been developed. With a finite-rate/eddy-dissipation model it was possible to well represent an experimental test case. Scaling of the empiric constant $A$ of the eddy-dissipation model by a factor of 10 was however necessary. Two different prechamber geometries have been tested to assess their respective combustion performance. The small cylindrical prechamber has shown to be too small to properly ignite the main chamber. The mixture formation in the cylindrical-conical prechamber geometry is more favourable for a homogeneous ignition. The combustion timing and duration are well represented in the simulations. An overall energy balance of the simulation is in good agreement with the experimental case. The combustion was complete for the simulations, thus under predicting the unburned hydrocarbon emissions. The numerical model can be used to guide future design modifications of the prechamber engine. Further work might be carried out on validating the scaled model with further experimental data. A full engine cycle simulation would be necessary to completely compare the energy balances. The model could be used to investigate the influence of cycle-by-cycle fluctuations on the combustion timing that were observed during the experiments.

## 5 Acknowledgements

This project has been financially supported by the Swiss National Science Foundation (subsidy number 200020-105487).

## References

[1] R.P. Roethlisberger, D. Favrat, Comparison between direct and indirect (prechamber) spark ignition in the case of a cogeneration natural gas engine, Part I&II. Applied Thermal Engineering 22 (11) (2002) 1217-1243.

[2] R.P. Roethlisberger, D. Favrat, Investigation of the prechamber geometrical configuration of a natural gas spark ignition engine for cogeneration, Part I&II. International Journal of Thermal Sciences 42 (3) (2003) 223-253.

[3] A. Roubaud, D. Favrat, Improving performances of a lean burn cogeneration biogas engine equipped with combustion prechambers. Fuel 84 (16) (2005) 2001-2007.

[4] S. Heyne, M. Meier, B. Imbert, D. Favrat, Experimental investigation of prechamber autoignition in a natural gas engine for cogeneration, accepted for publication in Fuel.

[5] S. Aceves, D. Flowers, J. Martinez-Frias, J.R. Smith, C.K. Westbrook, W. Pitz et al., A sequential fluid-mechanic chemical-kinetic model of propane HCCI combustion. SAE technical paper 2001-01-1027, 2001.

[6] S.C. Kong, A study of natural gas/DME combustion in HCCI engines using CFD with detailed chemical kinetics. Fuel 86 (10-11) (2007) 1483-1489.

[7] Q.P. Zheng, H.M. Zhang, D.F. Zhang, A computational study of combustion

in compression ignition natural gas engine with separated chamber. Fuel 84 (12-13) (2005) 1515-1523.

[8] G.P. Smith, D.M. Golden, M. Frenklach, N.W. Moriarty, B. Eiteneer, M. Goldenberg et al., GRI Mech 3.0. `http://www.me.berkeley.edu/gri\_mech/releases.html`; 2002.

[9] D. Wunsch, S. Heyne, J.B. Vos, D. Favrat, Numerical flow simulation of a natural gas engine equipped with an unscavanged auto-ignition prechamber. Proceeding from the 3rd European Combustion Meeting, 2007.

[10] A. Turbiez, A. El Bakali, J.F. Pauwels, A. Rida, P. Meunier, Experimental study of a low pressure stoichiometric premixed methane, methane/ethane, methane/ethane/propane and synthetic natural gas flames. Fuel 83 (7-8) (2004) 933-941.

[11] B. Magnussen, H. Hjertager, On mathematical modeling of turbulent combustion with special emphasis on soot formation and combustion. Proceedings of the Combustion Insitute (1976) 719-29.

[12] J.B. Heywood. Internal combustion engine fundamentals. McGraw-Hill International Editions, Automotive Technology Series, 1988.

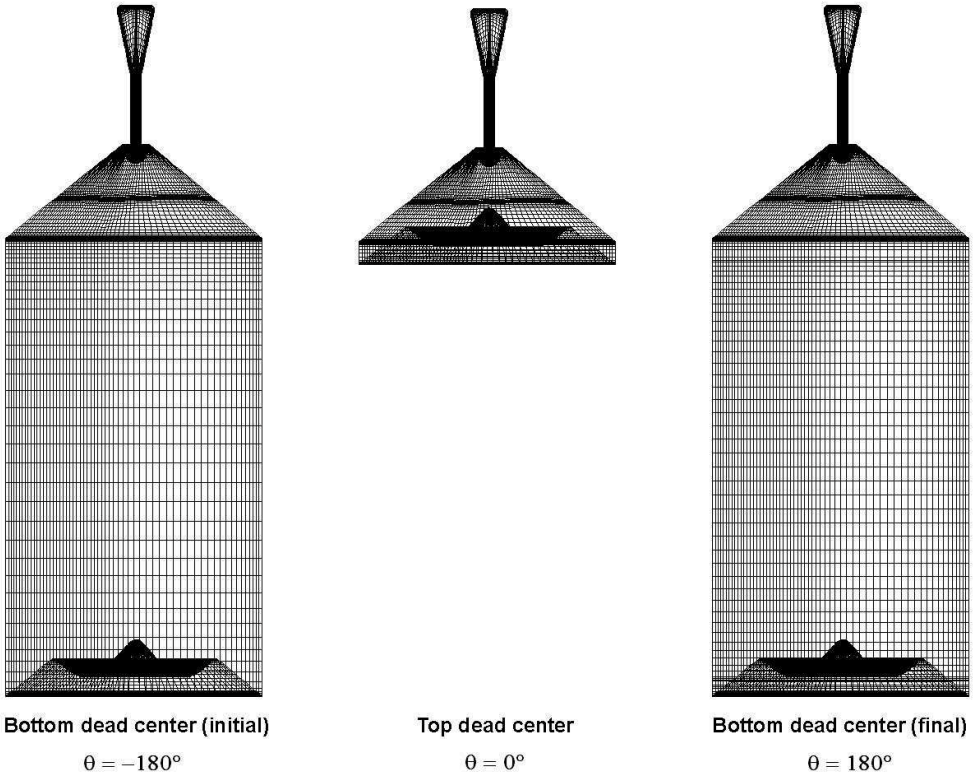


Fig. 1. Computational mesh for original prechamber geometry.

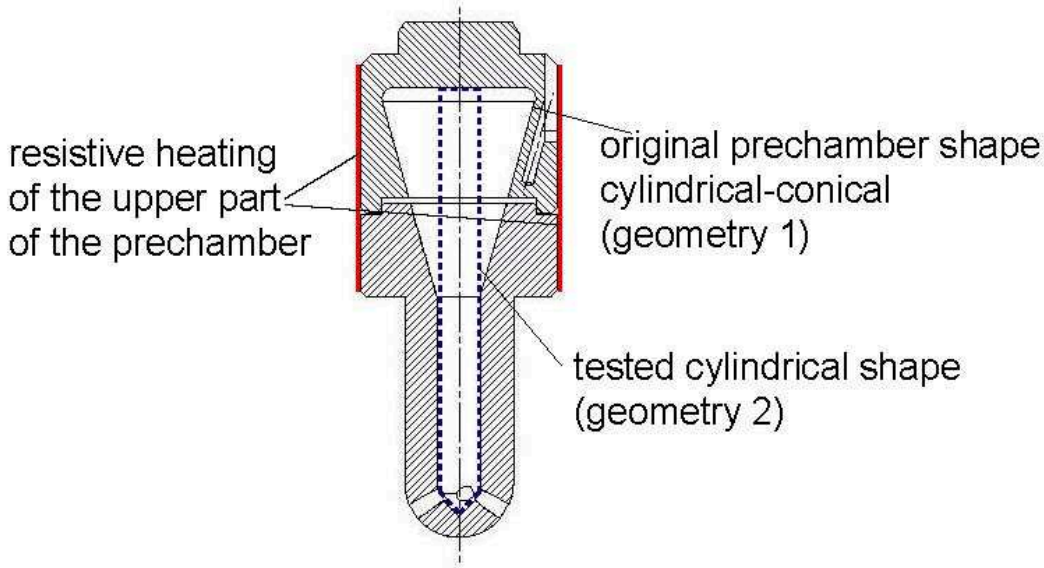


Fig. 2. Original prechamber(geometry 1) and cylindrical prechamber (geometry 2) shape.

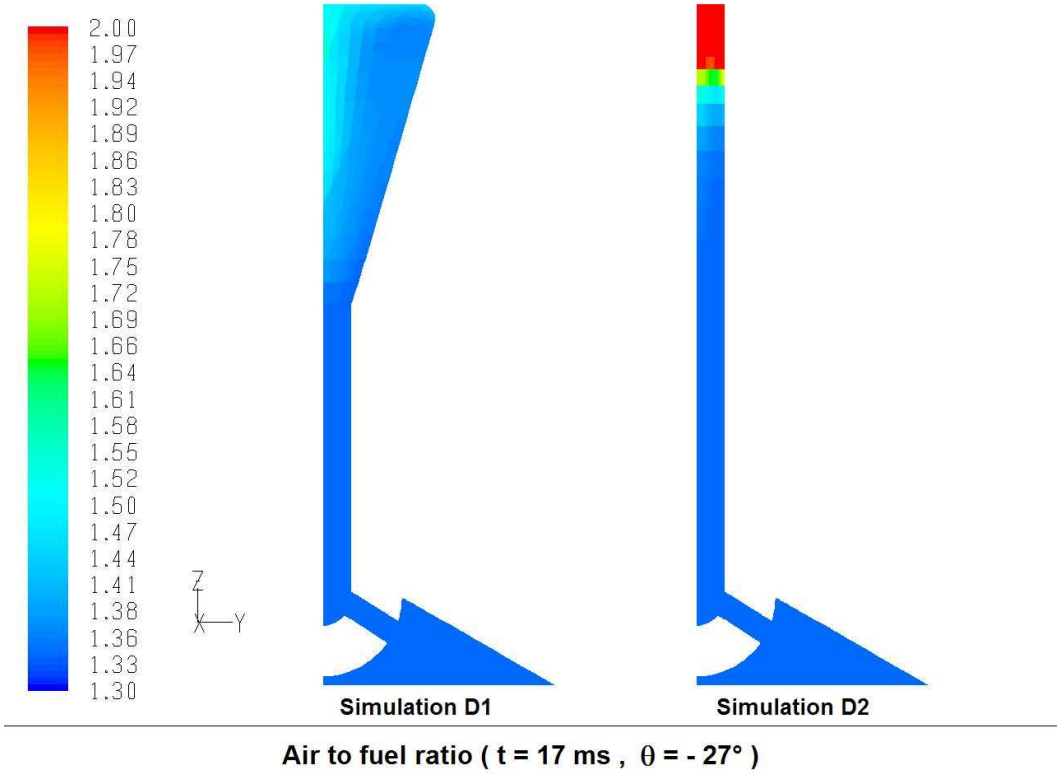


Fig. 3. Lambda distribution for both prechamber geometries. Simulations D1 and D2.

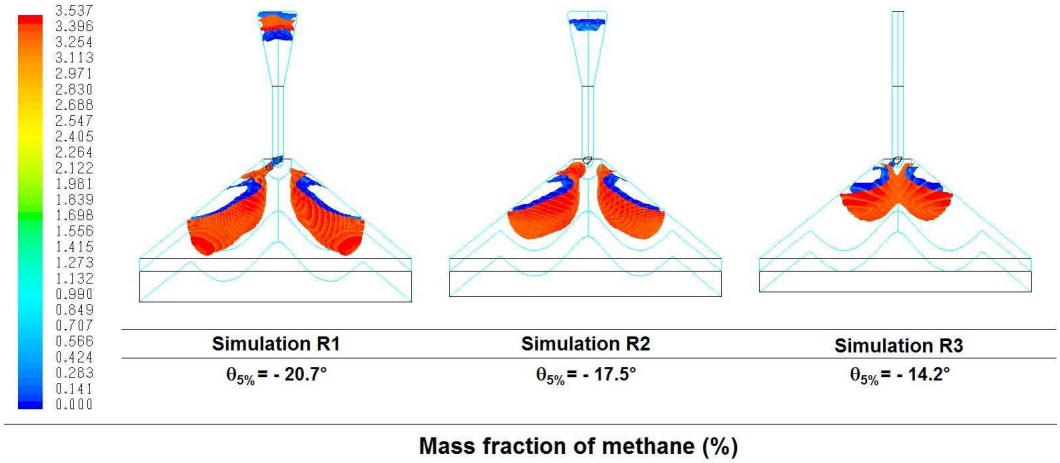


Fig. 4. Flame front at 5% heat release for simulations R1,R2 and R3. Iso-surfaces for 95% of initial $CH_4$ concentration (red) and 10% of initial $CH_4$ concentration (blue).

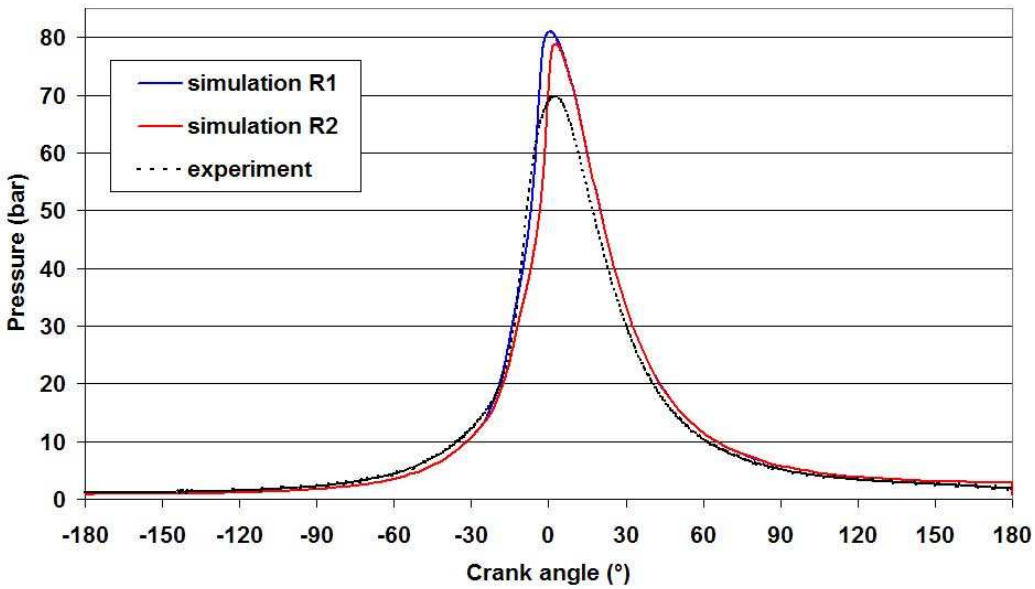


Fig. 5. Pressure curve for simulations R1 and R2 in comparison to the experimental pressure curve.

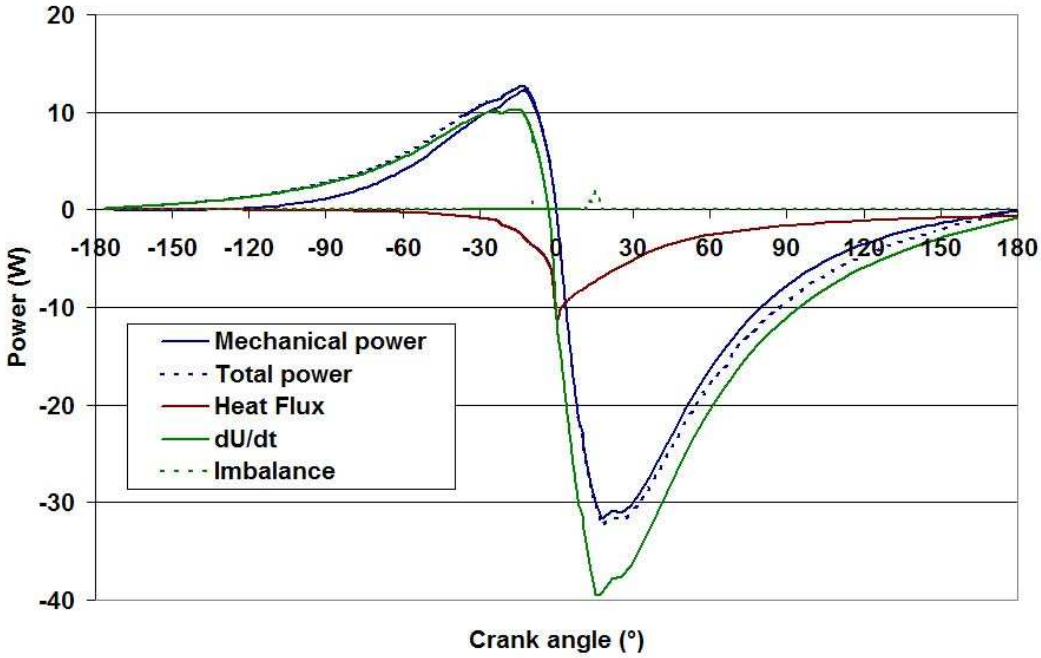


Fig. 6. Instantaneous energy balance for simulation R2.

Table 1
Engine dimensions and simulated experimental conditions.

| | |
|---|---|
| Bore [mm] | 95.25 |
| Stroke [mm] | 114.3 |
| Piston rod length [mm] | 222.25 |
| Compression ratio $\epsilon$ | 13 |
| RPM [$\mathrm{min}^{-1}$] | 1500 |
| Relative air-to-fuel ratio $\lambda$ | 1.3 |
| Natural gas composition | $CH_4/C_2H_6/C_3H_8/CO_2/N_2$ |
| (mole-%) | 90.3/5.2/1.1/1.1/2.3 |

Table 2
Simulated cases for the two prechamber geometries.

| Simulation | Abbreviation | Geometry |
|---|---|---|
| Non-reactive with burnt gases in prechamber | D1 | 1 |
| Non-reactive with burnt gases in prechamber | D2 | 2 |
| Reactive with homogeneous gas phase | R1 | 1 |
| Reactive with burnt gases in prechamber | R2 | 1 |
| Reactive with homogeneous gas phase | R3 | 2 |

Table 3
Boundary and initial conditions for the simulations (in parenthesis: prechamber gas phase composition and temperature for simulations D1,D2 and R2). Based on the experimental test case (engine speed 1500 $min^{-1}$, relative air-to-fuel ratio $\lambda = 1.3$, compression ratio CR=13.

| Boundary conditions | |
|---|---|
| Main chamber wall temperature (K) | 376 |
| Prechamber wall temperature (K) | 793.2 |
| **Initial conditions** | |
| Mass fraction (%) | |
| $CH_4$ | 3.537 (0) |
| $C_2H_6$ | 0.320 (0) |
| $C_3H_8$ | 0.100 (0) |
| $CO_2$ | 1.018 (11.96) |
| $H_2O$ | 0.725 (9.41) |
| $O_2$ | 20.93 (5.626) |
| $N_2$ | 73.37 (73.37) |
| Pressure (bar) | 0.86 |
| Temperature (K) | 353.4 (718) |
| Turbulent kinetic energy (m2/s2) | 5 |
| Turbulent dissipation rate (m2/m3) | 1000 |

Table 4
Ignition and combustion timing for the experiment and the different simulations.

| | $\theta_{5\%}$ | $\theta_{90\%}$ | $\Delta_{combustion}$ | $\Delta_{ignition}$ |
|---|---|---|---|---|
| Experiment | -18° | -2° | 16° | - |
| Simulation R1 (Geometry 1) | -20.7° | -2.9° | 17.8° | 4.3° |
| Simulation R2 (Geometry 1) | -17.5° | 0.6° | 18.1° | 5.1° |
| Simulation R3 (Geometry 2) | -14.2° | 9.3° | 23.5° | 16.3° |

Table 5
Overall energy balance. Experimental and simulated values. Orders of magnitude indicated in literature[12].

| | $\dot{E}_{total}$ | $P_{brake}$ | $\dot{Q}_{total}$ | $\dot{E}_{exhaust}$ | $\dot{E}_{unburnt}$ |
|---|---|---|---|---|---|
| Experiment (W) | 17890 | 5814 | 6368 | 4586 | 1122 |
| % $\dot{E}_{total}$ | 100 | 32.5 | 35.6 | 25.6 | 6.3 |
| Simulation R2 (W) | 17890 | 7636 | 10254 | | $\approx 0$ |
| % $\dot{E}_{total}$ | 100 | 42.7 | 53.3 | | $\approx 0$ |
| Literature values (%) | 100 | 25-38 | 18-41 | 22-45 | 1-5 |